Fall 2022

An Investigation of the Relationship of Wave Intensity and Byssal Thread Strength of the Mussel Mytilus Californianus

Felicia M. Miller
San Jose State University

AN INVESTIGATION OF THE RELATIONSHIP OF WAVE INTENSITY AND BYSSAL THREAD STRENGTH OF THE MUSSEL *MYTILUS CALIFORNIANUS*

A Thesis

Presented to

The Faculty of Moss Landing Marine Laboratories

San José State University

In Partial Fulfillment

of the Requirements for the Degree

Master of Science

by

Felicia Miller

December 2022

The Designated Thesis Committee Approves the Thesis Titled

AN INVESTIGATION OF THE RELATIONSHIP OF WAVE INTENSITY AND BYSSAL THREAD STRENGTH OF THE MUSSEL *MYTILUS CALIFORNIANUS*

by

Felicia Miller

APPROVED FOR MOSS LANDING MARINE LABORATORIES

SAN JOSÉ STATE UNIVERSITY

December 2022

Jonathan Geller, Ph.D.	Moss Landing Marine Laboratories
Amanda Kahn, Ph.D.	Moss Landing Marine Laboratories
Thomas Connolly, Ph.D.	Moss Landing Marine Laboratories

ABSTRACT

AN INVESTIGATION OF THE RELATIONSHIP OF WAVE INTENSITY AND BYSSAL THREAD STRENGTH OF THE MUSSEL *MYTILUS CALIFORNIANUS*

By Felicia Miller

The intertidal zone is a stressful environment with one of the main stressors being the fluctuation of wave energy over time and space. A structural adaptation employed by mussels living within the intertidal zone is byssal threads that aid in attachment while dealing with various levels of wave exposure. The California mussel, *Mytilus californianus*, lives in extremely wave exposure conditions, which makes it a great study species to assess the relationship between wave intensity and byssal thread strength. In this study, *Mytilus californianus* were collected from two locations in the Monterey Bay, each with a predicted wave exposed site and a wave protected site. The dimensions of the byssal threads were recorded and the threads tensile strength were measured on a tensometer. Thread strength and thickness were higher at the wave exposed site in Santa Cruz compared to the wave protected site. At the other location, Pacific Grove, there was no difference between the predicted exposed and protected sites, but thread strength and thickness increased over time, mirroring seasonal changes in wave energy. These results support the relationship between wave intensity and thread strength and thickness over space and time, but the response to variable wave intensity is not consistent at both locations. A more accurate wave intensity assessment for individual mussels would be helpful to determine the intricacies of this relationship moving forward.

ACKNOWLEDGMENTS

I want to thank many people for their support and help with my thesis. My advisor Dr. Jonathan Geller not only funded the first few semesters of my time in the Moss Landing Marine Laboratories Graduate program, but also employed me for the entirety of my time at Moss Landing. Jon was instrumental in the composition of my thesis and helping me weave together a cohesive research story. My committee member Dr. Amanda Kahn helped keep the joy of science alive during this writing and research process and Dr. Tom Connolly helped with all of my instrument issues in the field. A big thank you to Dr. Emily Carrington who allowed me to have access to her tensometer, without which I would not have been able to collect a majority of my data. I would also like to thank my family and friends who helped carry me to the end of this program.

TABLE OF CONTENTS

LIST OF TABLES

LIST OF FIGURES

GLOSSARY OF TERMS

Strain (ε): the change in length of specimen during tensile test divided by the specimen length at rest

Stress (σ): the force a specimen experiences divided by the specimen's cross-sectional area

Extendibility: the change in length of specimen

Elasticity: the ability of a specimen to be pulled to a stress value and then when the stress is removed, the specimen is able to return to original shape without permanent damage

Introduction

The rocky intertidal zone is one of the most punishing habitats and requires organisms to overcome desiccation, submersion, solar radiation, and varying degrees of wave exposure. Impact by waves is the major mechanical force endured by intertidal organisms that has the potential to cause damage or dislodgement. An adaptation to overcome wave-induced dislodgment employed by mussels (bivalves in the family Mytilidae) are byssal threads. Byssal threads are proteinaceous filaments that anchor a mussel to the rock surface for attachment and resistance to wave stress. The byssal threads produced by the mussel act as a holdfast in which multiple threads, each attached to the rock surface by an adhesive plaque, are joined into a singular stem rooted in the mussel's foot tissue. This entire structure including the root, stem, threads and adhesive plaque is called the byssus (Brown, 1952).

The tenacity (attachment strength controlled for body size) of the mussel byssus fluctuates in response to a variety of factors in nature including seasonal wave action and reproductive cycles, and also varies among mussel species (Carrington, 2002; Bell and Gosline, 1997; Witman and Suchanek, 1984). Tenacity of the mussel byssus is measured by calculating the force needed to dislodge the entire mussel from the substrate. This measurement considers the cumulative attachment strength of all the byssal threads of an individual mussel and their anchor in tissue and adhesion to rock. The byssus of *Mytilus edulis* increase in tenacity two-fold in the late winter and early spring in Rhode Island when compared to the summer months (Carrington, 2002). This pattern of tenacity mirrors a seasonal increase in wave action. The reproductive cycles of mussels may also impact mussel tenacity through the allocation of energy. *Mytilus edulis* spawn in the late summer, allowing for a greater proportion of energy to be allocated to byssal thread production in the fall and winter months. Gamete development in early spring demands more energy which may be redirected from byssal thread production and result in a decline of tenacity (Carrington, 2002). Different species of mussels have different ranges of byssal thread strength. *Mytilus californianus* has thicker byssal threads compared to *M. edulis* (Witman and Suchanek, 1984) and *M. trossulus* (Bell and Gosline, 1997), resulting in greater tenacity and the ability to persist in wave-exposed habitats and outcompete other species of mussels (Bell and Gosline, 1997). *Mytilus californianus* has also been observed to produce byssal threads while exposed to air at low tide which might be a unique adaptation to the high wave intensities where the species tend to live (Bell and Gosline, 1997).

While tenacity measurements evaluate the strength and attachment of the entire byssus, individual byssal thread strength varies based on the species of mussel and the region of the thread where force is applied. Tensile testing is often conducted by a tensometer which can determine thread mechanical properties, such as the amount of stress and strain threads can endure and elasticity. The distal region of a thread has 5-50 fold greater initial stiffness and is twice as strong as the proximal region (Bell and Gosline, 1996) while the proximal region has twice the extendibility of the distal region for the species *Mytilus californianus, M. trossulus,* and *M. galloprovincialis* (Bell and Gosline, 1996). Although force-extension or stress-strain curves indicate that mechanical properties are similar for threads from a wide range of byssate species, the magnitude of these parameters can vary (Bouhlel et al., 2017; Brazee and Carrington, 2006; Bell and Gosline, 1996). The strain, stress, and elasticity of the distal region of byssal threads from different bivalve molluscs, including the mussels *M. edulis*, *M. galloprovincialis*, *M. californianus*, *Perna perna*, *Xenostrobus securis*, *Brachidontes solisianus,* the pen shell *Pinna nobilis*, and the oyster *Isognomon bicolor*, are specific to each species, with *M. californianus* having the highest strength and stiffness and *P. nobilis* having the lowest, potentially due to its sandy subtidal habitat (Bouhlel et al., 2017).

Although tensile tests provided comparative information about the mechanical properties of individual byssal threads, they were typically used on byssal threads produced from mussels in lab. Some studies utilize tensile tests on byssal threads taken from nature (e.g. Babarro and Carrington, 2011), but this is not a common practice. Studies examining the effect of environmental conditions on mussel attachment tended to use tenacity measurements instead of tensile tests because their goal was to assess the dislodgement of the mussel from the substrate.

The mechanical properties of byssal threads are due to their complex protein composition. Byssal threads are formed when three glands secrete proteins into a groove located in the foot through a process similar to injection molding. Byssal threads are made up of three regions: the proximal region, the distal region, and the adhesive plaque (Brown, 1952). The proximal region is connected to the stem of the byssus and ends about halfway down the thread. The distal region continues from the proximal region and ends at the adhesive plaque. These two regions are differentiated by physical properties, structural organization, and protein components. The proximal region is characterized by its elasticity and is thicker in diameter than the distal region, in most mytilid species, due to the presence of internal coiled fibers (Qin and Waite, 1995). The distal region is stiffer and is typically thinner than the proximal region because the fibers in this region are less coiled (Lucas et al., 2002; Bell and Gosline, 1996; Qin and Waite, 1995). The core of the thread is made up of collagen-like proteins (preCols) and thread matrix proteins (TMP) (Wang and Scheibel, 2018). There are different types of preCols arranged within the thread regions and each have distinct characteristics. The proximal region consists mainly of preCol-P which has a flanking domain that is similar to elastin or resilin giving the thread region its elastic properties. The distal region consists mainly of preCol-D which has a flanking domain that is similar to silk, making this region rigid and tough (Qin et al., 1997; Qin and Waite, 1995). These preCols are arranged in complementary gradients along the thread and a separate collagen-like protein called preCol-NG spans the whole thread, helping to stabilize the core fibers (Qin and Waite, 1995). The thread is also coated by a cuticle made up of mussel foot protein-1 (MFP-1) that gives the thread its waterproof properties.

Byssal threads are capable of self-healing after dealing with wave force by using reversible metal chelate bonds. The metal binding regions can be found on the N- and C- terminus of the preCols in the core of the byssal thread (Vaccaro and Waite, 2001; Harrington and Waite, 2007). Each preCol is made up of a collagen-like domain with flanking regions unique to each type of preCol. At the end of these flanking regions are the N- and C-terminus where the metal chelate binding takes place. In preCol-D and preCol-P, these terminal regions are histidine rich and various metals can cross-bind these histidines to stabilize the byssal thread structure (Harrington et al., 2009; Harrington and Waite, 2007; Waite et al., 1998). Several different metals that can bind in this region including Zn^{2+}, Cu^{2+}, and Fe^{2+} (Vaccaro and Waite, 2001; Waite et al., 1998). In preCol-NG, the terminal regions are glycine rich and metal ions are hypothesized to bind to glycine (Harrington and Waite, 2007). As the thread undergoes tension, the metal chelate bonds break but will readily reform after that tension event passes. Metal binding sites are also found in the cuticle of the byssal thread (Harrington et al., 2010). Within the cuticle, metal ions, mainly Fe^{3+}, binds to 3,4-dihydroxyphenylalanine (dopa) (Harrington et al., 2010; Sun and Waite, 2005), which is a post-translational modification of tyrosine. The cuticles of both *Mytilus californianus* and *M. galloprovincialis* have granules with a higher density of dopa compared to the surrounding thread cuticle matrix (Harrington et al., 2010). The concentration of dopa-Fe complexes within the granule give the cuticle its stiffness, while the areas around the granules with less concentrated dopa allow the cuticle to also be elastic (Harrington et al., 2010).

Mussel byssal threads have been studied extensively, but most of the research has been concentrated either on the impact of environmental conditions on the whole mussel byssus or the molecular makeup of individual byssal threads. Few studies have taken an integrative approach and focused on the influence of environmental factors on the structure and strength of the individual byssal threads. In this study, I explored the adaptability of the byssal threads and the impact of wave exposure has on the mechanical and morphological characteristics of mussel byssal threads.

Research Questions and Hypotheses:

In my thesis, I determined if *M. californianus* byssal threads from wave exposed sites were different from wave protected sites by comparing their strength, size, and structure.

Question 1: Does byssal thread tensile strength differ at sites with various levels of wave exposure?

Hypothesis 1: *B*yssal thread tensile strength is higher at wave exposed sites and lower at wave protected sites.

Question 2: Do byssal thread regional diameters differ at sites with various levels of waves exposure?

Hypothesis 2: *B*yssal thread diameters will be larger in wave exposed habitats than in wave protected habitats.

Methods

Collection Sites

M. californianus were collected from sites in Pacific Grove and Santa Cruz, CA. Each location had two collection sites. The Santa Cruz sites were Lighthouse Field State Beach (36°57'05.4"N, 122°01'53.4"W) and Cowell Beach (36°57'31.3"N, 122°01'32.2"W). The Pacific Grove sites were Pacific Grove Marine Gardens (36°38'15.2"N, 121°56'07.0"W) and Point Cabrillo. These sites were selected because in each location there was a predicted exposed site, Lighthouse Field Beach and Pacific Grove Marine Gardens, and a protected site, Cowell Beach and Point Cabrillo. The level of exposure was estimated using wave height data generated by a United States Geography Survey (USGS) wave model. The USGS wave model used bathymetric data for the California Seafloor Mapping Program Project to simulate wave propagation along continental shelf off the California coast (Erikson et al., 2014). To verify the level of wave exposure at each site, maximum wave velocity over a given time period was measured using dynamometers (Bell and Denny, 1994) (Appendix). Some of these dynamometers became dislodged during the span of collection dates resulting in gaps in the wave velocity data. The California coastal wave monitoring and prediction system (MOPs model) (O'Reilly et al., 2016) was used to verify the wave velocities recorded by the dynamometers and to fill in the missing data. The MOPs model estimates nearshore wave conditions using offshore buoys in California.

Wave Model

The California coastal wave monitoring and prediction system (MOPs model) (O'Reilly et al., 2016) was used to assess near shore wave conditions, at a depth of 20 m, around the collection sites. The MOPs model estimated nearshore wave conditions using offshore deep-water directional wave buoys and these estimates were validated by nearshore buoys. The MOP model was developed to be used for regional sediment management and nearshore process modeling in San Clemente, California and then expanded to estimate near shore conditions along the whole coast of California. Model accuracy was determined using the R-squared coefficient of determination ("model skill"). MOPs model skill in estimating San Clemente's wave conditions was high because there were many near shore buoys specifically used for the development for the MOPs model. The San Clemente near shore environment is sandy and homogeneous, whereas rocky environments are found in the south of the Monterey Bay. The MOPs model developed for sandy environments may be less accurate in rocky places and indeed had moderate skill when estimating near shore wave conditions in Santa Cruz. The MOPs model was used to ground truth the dynamometer wave velocity measurements and fill in any missing data resulting from dislodged dynamometers. The parameter used to evaluate the exposure of the collection sites was significant wave height.

Mussel Collection

Mussels were collected on 4 dates for the Santa Cruz sites and on 3 dates for the Pacific Grove sites between July 2019 and February 2020. During collection events, 25-30 *M. californianus* were collected from mussel beds. Mussels were collected from horizontally oriented beds and mussels at the edge of the beds or solitary mussels were selected for ease of access and because edge and solitary mussels would not be shielded by other mussels to wave forces like mussels within a bed. Mussels were removed by scraping byssal threads off the substrate with a scalpel to keep the threads with plaque intact. Measurements taken for each mussel included length, maximum width, maximum thickness, and wet weight (Figure 1).

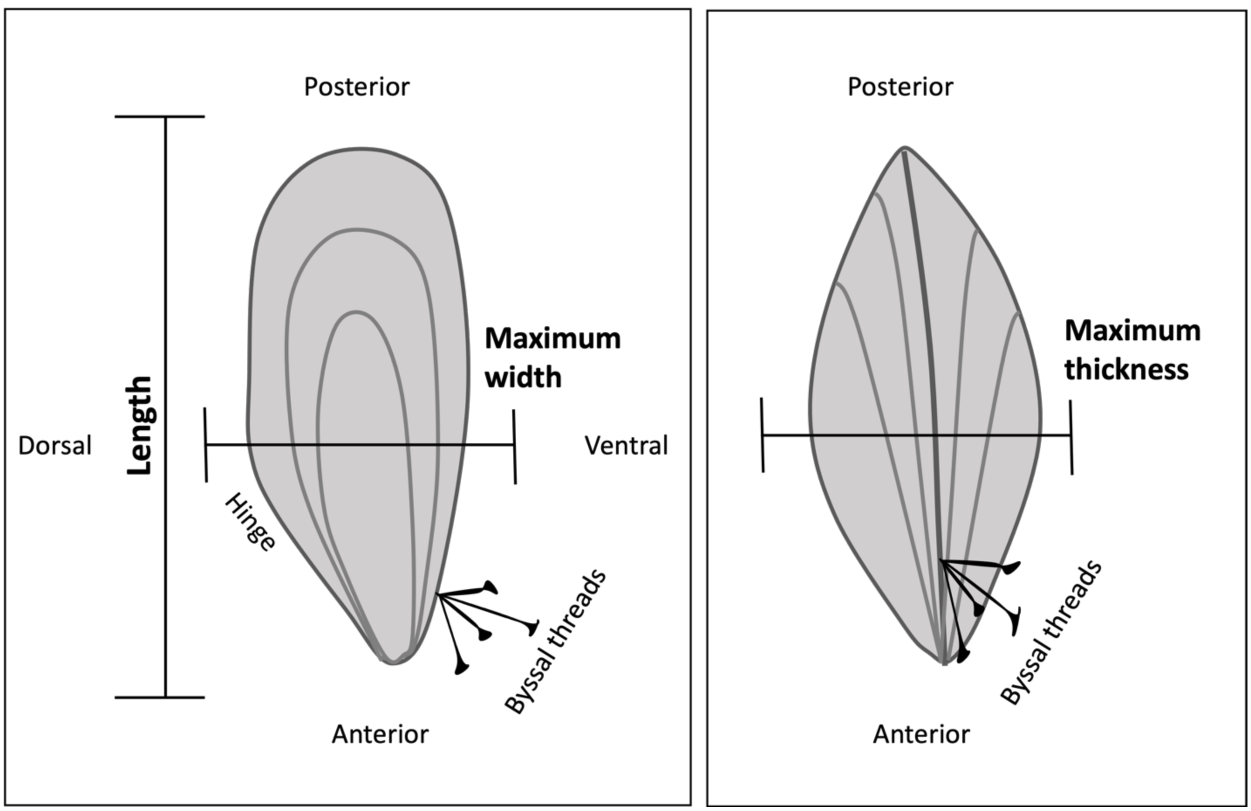

Figure 1. Mussel measurements recorded in study. Mussel measurements include length, maximum width, and maximum thickness.

Mussels were then euthanized by freezing and left in the freezer to be dissected later. Later, mussels were defrosted, the entire byssus was dissected out of each mussel and the total number of byssal threads were counted. Byssal threads were left to dry out and stored dry until processed. The byssal threads underwent a series of analyses to assess their strength and structure.

Tensometer

Tensile strength of byssal threads was measured to gauge their reaction to applied forces. From each collection event, 8-10 mussels for each site had one byssal thread selected to be tested using an Instron-5565 tensometer (Illinois Tool Works Inc., Norwood, MA, USA) at Friday Harbor Laboratories. In preparation for the tensile testing, the entire byssus of the mussel was soaked in filtered sea water, then one thread near the stem's midpoint with an intact plaque and no noticeable damage was chosen for testing. All other threads were trimmed away from the stem of the byssus, leaving only the thread to be tested. The stem of the byssus was glued between pieces of cardstock with cyanoacrylate (Loctite Gel Control Super Glue, Henkel Consumer Adhesives, Avon, NY, USA) taking care not to get any glue on the proximal region of the thread. The distal end of the thread was also glued between cardstock. These pieces of cardstock were held in the pneumatic grips of the tensometer. Byssal threads were subjected to crosshead speeds of 10 mm min^{-1} (Bell and Gosline, 1996) until completely pulled apart. While undergoing the tensile test, the thread and grips were submerged in filtered sea water (Figure 2).

Data from threads that broke close to the grips were disregarded because the breakage most likely resulted from damage to the thread, as determined by a significantly shorter tensile test of less than 2 seconds. The tensometer and

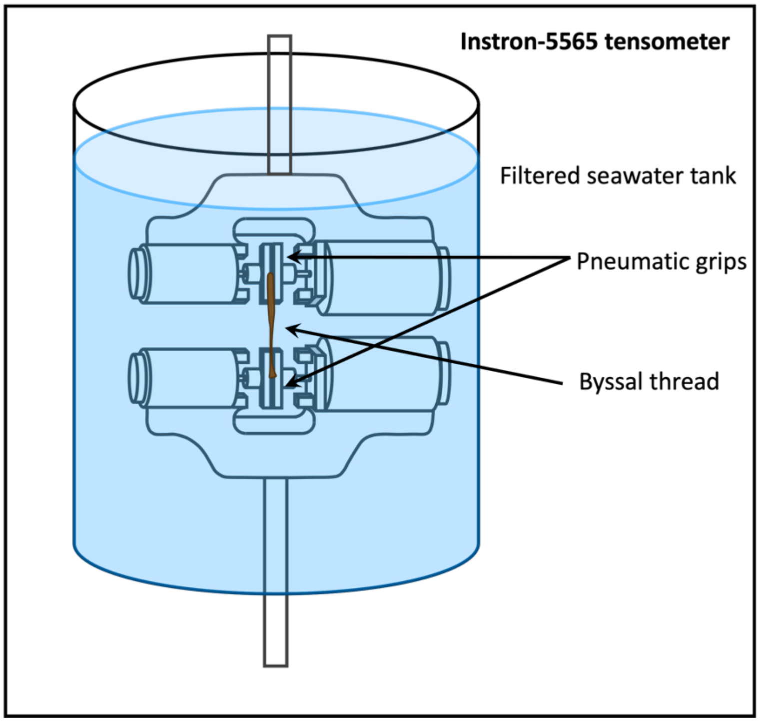

Figure 2. Diagram of the sample holder on a tensometer used for tensile tests.

connected computer interface measured thread extension (mm) and the load applied to the thread (N). These measurements were used to calculate the thread's stress (σ), strain (ε), ultimate stress (σ_{max}), and ultimate strain (ε_{max}).

Thread Morphometrics

Dimensions of the byssal threads were taken using a stereomicroscope M5 (Wild Heerbugg, Switzerland) fitted with optical micrometer to determine if there was a difference in diameter of thread regions from mussels collected from areas with different levels of wave exposure. After threads were tested on the tensometer, their dimensions were measured. The diameter of the proximal and distal thread regions and the length of the whole thread were measured. The cross-sectional area of the thread regions was calculated similarly to Bell and Gosline (1996) using

$$A = \pi r^2$$

where the cross sections of the thread sections will be assumed to be circular.

Results

Environmental Data

Three dynamometers were deployed at each site but as the wave forces increased from summer to winter, all dynamometers were dislodged. Further, there was no sampling time period in which dynamometers were retrieved in all sites, making it difficult to compare the maximum wave velocities of the sites and how they changed over time. The maximum wave velocity calculations from the dynamometers are included in Table 1.

Table 1. Dynamometer maximum wave velocity calculations. The date the dynamometer was deployed is the start date and the date the measurement was recorded is the end date. Point Cabrillo had two calculations over the same time period because two dynamometers were retrieved at that site.

Start date	End date	Site	Maximum wave velocity (m/s)
16 July 2019	1 Aug 2019	Pacific Grove Marine Gardens	5.46
31 July 2019	14 Aug 2019	Cowell Beach	5.82
1 Aug 2019	15 Aug 2019	Point Cabrillo	5.07
1 Aug 2019	15 Aug 2019	Point Cabrillo	6.17
1 Aug 2019	15 Aug 2019	Pacific Grove Marine Gardens	6.81

The MOP model was used in place of the dynamometer measurements to evaluate the wave exposure of the collection sites (Figure 3). The average daily wave height at Pacific Grove Marine Gardens exceeded those at Point Cabrillo for 100% of the days from March 2019 to March 2020. At the Santa Cruz sites the average daily wave height at Lighthouse Field Beach exceeded those at Cowell Beach for 100% of the days as well.

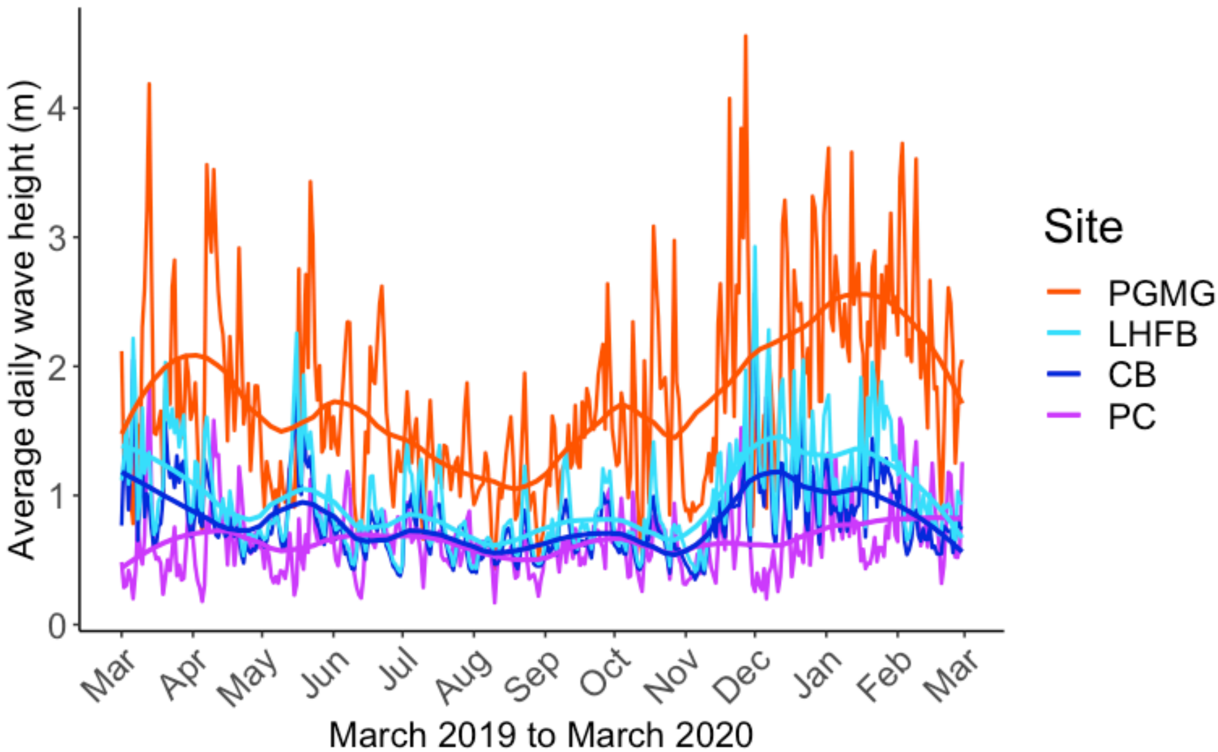

Figure 3. The fluctuating lines are the average daily wave height from all collection sites, including Santa Cruz sites Lighthouse Field Beach (LHFB) and Cowell Beach (CB) and Pacific Grove sites Pacific Grove Marine Gardens (PGMG) and Point Cabrillo (PC). Average daily wave heights were calculated from hourly wave heights predicted by MOPs model. The average daily wave height data was fitted using local polynomial regression fitting ("loess" method used for stat_smooth function from ggplot_2 r studio package) creating a smooth line for each site.

Thread Morphometrics

Thread morphometrics recorded include thread length, thread number, and thread proximal and distal diameter. Statistics comparing the thread morphometrics from Santa Cruz across sites and collection dates are included in Table 2a. Byssus proximal and distal diameter varied between the two Santa Cruz sites (2-way ANOVA, Proximal, $F_{1, 59} = 5.453$, $p < 0.05$; Distal, $F_{1, 59} = 6.704$, $p < 0.05$) (Figure 4a)

Table 2. Statistics results from a 2-way ANOVA looking at the difference in site, collection date, and the interaction of site and collection date for the thread morphometrics. Table 2a contains statistics for the Santa Cruz location and Table 2b contains statistics for the Pacific Grove location. In the P column, ns stands for not significant. MS stands for mean squares.

a.

Santa Cruz 2-Way ANOVA	df	MS	F	P
Proximal diameter				
Site	1	0.014	5.453	<0.05
Date	3	0.001	0.277	ns
Site x Date	3	0.003	1.396	ns
Residuals	59	0.002		
Distal diameter				
Site	1	0.019	6.704	<0.05
Date	3	0.001	0.103	ns
Site x Date	3	0.002	0.875	ns
Residuals	59	0.003		
Thread length				
Site	1	16.275	2.088	ns
Date	3	14.583	1.871	ns
Site x Date	3	4.914	0.63	ns
Residuals	59	7.794		
Thread number				
Site	1	733.8	0.992	ns
Date	3	1214.3	1.641	ns
Site x Date	3	1212.1	1.638	ns
Residuals	59	739.8		

b.

Pacific Grove 2-Way ANOVA	df	MS	F	P
Proximal diameter				
Site	1	0.002	1.084	ns
Date	2	0.023	11.784	<0.001
Site x Date	2	0.004	1.91	ns
Residuals	48	0.002		
Distal diameter				
Site	1	0.003	0.789	ns
Date	2	0.025	6.761	<0.01
Site x Date	2	0.003	0.919	ns
Residuals	48	0.004		
Thread length				
Site	1	9.996	2.045	ns
Date	2	18.12	3.707	<0.05
Site x Date	2	18.49	3.784	<0.05
Residuals	48	4.175		
Thread number				
Site	1	2589	0.839	ns
Date	2	10231	3.317	<0.05
Site x Date	2	10252	3.324	<0.05
Residuals	48	1711		

(Figure 4b) but there was no difference between the collection dates and no significant interaction between site and date collected. For both proximal and distal diameters, Lighthouse Field Beach had a significantly higher diameter than Cowell Beach.

Statistics comparing thread morphometrics from Pacific Grove across sites and collection dates are included in Table 2b. For threads from Pacific Grove, there was an interaction between site and collection date for thread length (2-way ANOVA, $F_{2, 48} = 3.784$, $p < 0.05$) (Figure 5c) and thread number (2-way ANOVA, $F_{2, 48} = 3.324$, $p < 0.05$) (Figure 5d). The average proximal diameter increased from the August (0.223 mm ± 0.041) to the October (0.252 mm ± 0.050) to the January (0.292 mm ±

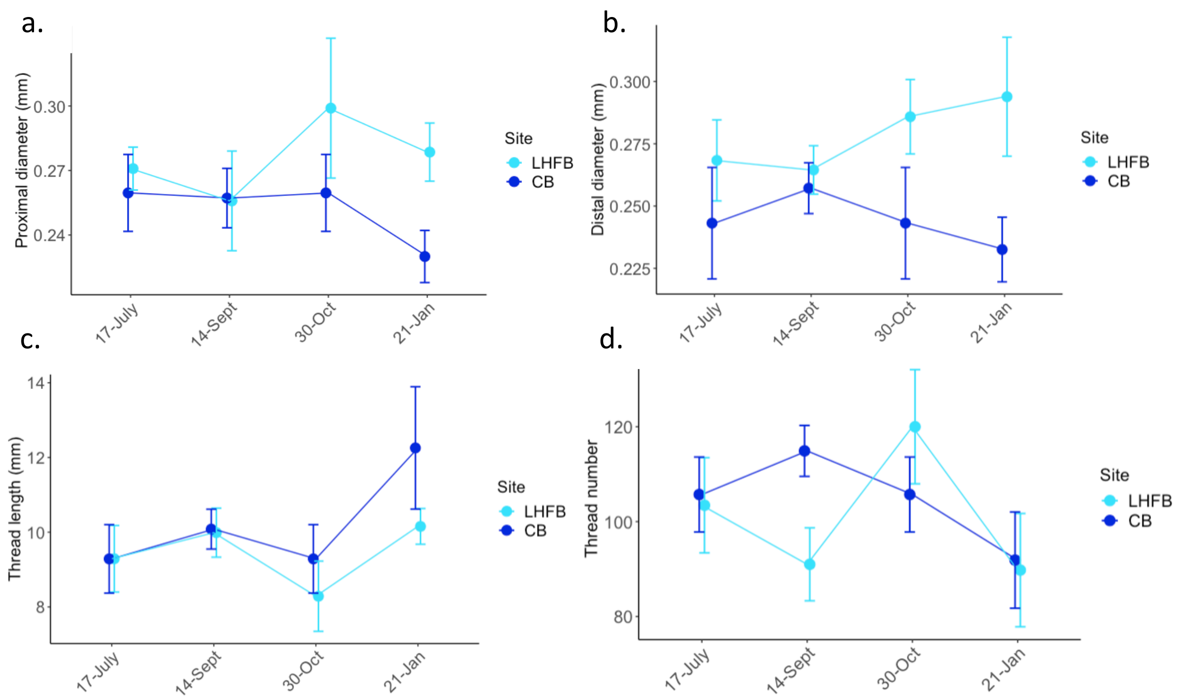

Figure 4. Santa Cruz thread morphometrics, including proximal diameter (a), distal diameter (b), thread length (c), and thread number (d). The mean and standard error are depicted for mussel collected at Lighthouse Field Beach and Cowell beach during each collection date.

0.044) collection dates, where the January proximal diameter was larger than both August and October (Tukey HSD, $p < 0.0001$, $p < 0.05$) (Figure 5a). A similar pattern was seen from the distal diameter measurements across the collection dates. Threads from January (0.304 mm ± 0.0678) had the largest distal diameter of the collection dates followed by those from the October collection date (0.257 mm ± 0.0602), and the August threads (0.233 mm ± 0.0520) had a significantly smaller diameter than the January threads (Tukey HSD, $p < 0.01$) (Figure 5b). The Pacific Grove byssal threads were longest in January (10.38 mm ± 2.632) followed by the August threads (8.988 mm ± 1.780) with the October threads (8.528 mm ± 2.483) dipping lower between the two other collections. The January thread length

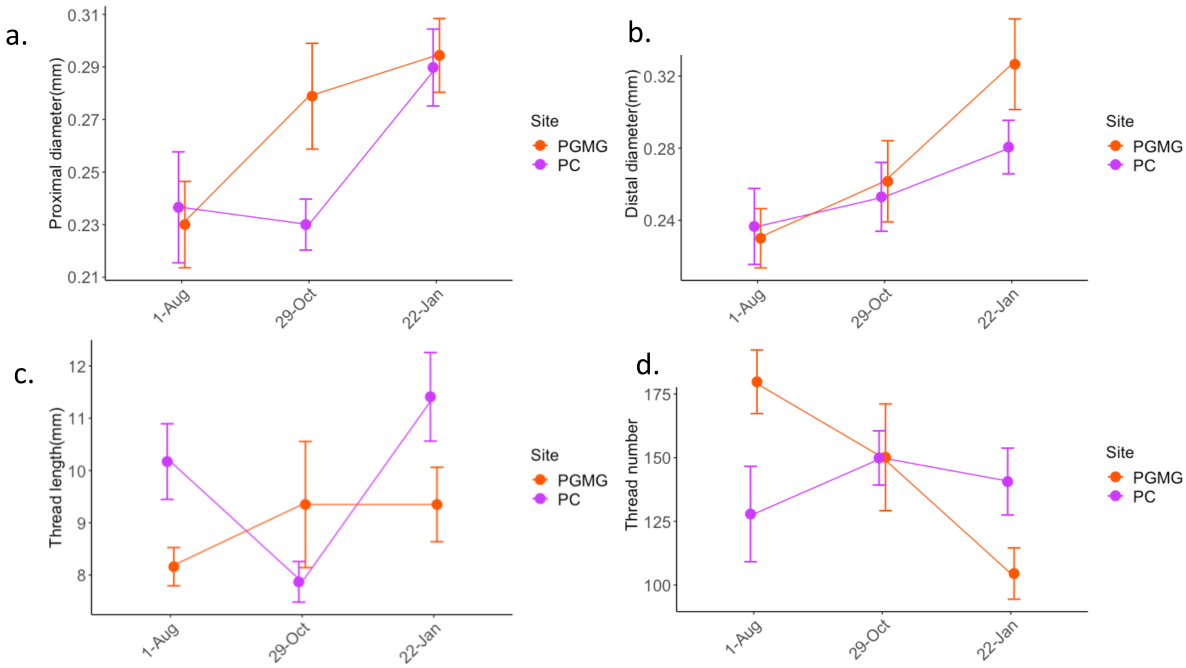

Figure 5. Pacific Grove thread morphometrics, including proximal diameter (a), distal diameter (b), thread length (c), and thread number (d). The mean and standard error are depicted for mussel collected at Pacific Grove Marine Gardens and Point Cabrillo during each collection date.

measurements were significantly longer than the October thread lengths (Tukey HSD, $p < 0.05$) (Figure 5c). The highest number of byssal threads was recorded in October (165.611 $\pm$ 77.934), followed by August (158.412 $\pm$ 49.934), and January (122.55 $\pm$ 40.499) with the smallest number of threads. The October collection date had a significantly larger number of byssal threads than in January (Tukey HSD, $p < 0.05$) (Figure 5d).

Tensometer

Tensometer parameters, including maximum load, breaking strain, and maximum stress, were measured for byssal threads from Santa Cruz sites and Pacific Grove sites (Table 3). Statistical tests comparing tensiometer parameters across site

Table 3. Mean and standard deviation of tensiometer parameters including maximum load, breaking strain, and maximum stress for the Santa Cruz sites, Cowell Beach (low wave exposure) and Lighthouse Field Beach (high wave exposure), and Pacific Grove sites, Point Cabrillo (low) and Pacific Grove Marine Gardens (high).

Site	Maximum load (N)	Breaking strain	Maximum stress (MPa)
Santa Cruz			
Cowel Beach	1.577 ± 0.542	1.138 ± 0.384	29.052 ± 15.878
Lighthouse Field Beach	2.009 ± 0.709	1.255 ± 0.358	27.37 ± 10.027
Pacific Grove			
Point Cabrillo	1.696 ± 0.668	1.128 ± 0.298	26.765 ± 8.787
Pacific Grove Marine Gardens	1.845 ± 0.724	1.207 ± 0.312	28.861 ± 15.695

and collection date are included in Table 4a for Santa Cruz and Table 4b for Pacific Grove. For the Santa Cruz sites, maximum load sustained by byssal threads varied significantly by site (2-way ANOVA, $F_{1, 59} = 7.626$, $p < 0.05$), with threads from Lighthouse Field Beach having a higher maximum load than threads from Cowell Beach. There was no significant difference for breaking strain and maximum stress between the Santa Cruz sites. Neither collection date nor interaction between site and date had a significant effect for any tensiometer parameters at the Santa Cruz sites.

For threads collected at the Pacific Grove sites, Pacific Grove Marine Gardens and Point Cabrillo, there was no significant difference in maximum load sustained, however maximum load varied significantly by date. The threads from January (2.187 N ± 0.611) had a significantly higher maximum load than both August (1.503 N ± 0.611) and October (1.564 N ± 0.486) collection dates (Tukey HSD, $p < 0.01$, $p < 0.05$). There was no significant difference in the breaking strain and maximum stress between sites or between collection dates.

Table 4. Statistics results from a 2-way ANOVA looking at the difference in site, collection date, and the interaction of site and collection date for the tensiometer parameters, including maximum load, breaking strain, and maximum stress. Table 4a contains statistics for the Santa Cruz location and Table 4b contains statistics for the Pacific Grove location. In the P column, ns stands for not significant. MS stands for mean squares.

a.

Santa Cruz 2-Way ANOVA	df	MS	F	P
Maximum load				
Site	1	3.130	7.626	<0.05
Date	3	0.168	0.41	ns
Site x Date	3	0.358	0.873	ns
Residuals	59	0.410		
Breaking strain				
Site	1	0.231	1.671	ns
Date	3	0.142	1.024	ns
Site x Date	3	0.135	0.977	ns
Residuals	59	0.138		
Maximum stress				
Site	1	47.39	0.267	ns
Date	3	108.37	0.61	ns
Site x Date	3	244.31	1.375	ns
Residuals	59	165.83		

b.

Pacific Grove 2-Way ANOVA	df	MS	F	P
Maximum load				
Site	1	0.305	0.741	ns
Date	2	2.758	6.708	<0.01
Site x Date	2	0.048	0.116	ns
Residuals	48	0.420		
Breaking strain				
Site	1	0.087	0.886	ns
Date	2	0.043	0.439	ns
Site x Date	2	0.017	0.177	ns
Residuals	48	0.099		
Maximum stress				
Site	1	58.45	0.352	ns
Date	2	216.86	1.308	ns
Site x Date	2	132.12	0.797	ns
Residuals	48	165.83		

After controlling for the thread morphometrics, including distal diameter, proximal diameter, thread length, and thread number, the significant difference in maximum load across collection dates remained (Table 5). For all of the mussel morphometric measurements from Pacific Grove, the maximum load from January was larger than both the October and August maximum loads. Also, the October collection dates had a higher maximum load than the August collection date. After controlling for the proximal diameter of the Santa Cruz threads, the site difference in the maximum load of the threads remained significant but the proximal diameter did not (ANCOVA, Site $F_{1, 61} = 6.223$, $p < 0.05$; Proximal diameter $p > 0.05$). Controlling for distal diameter, site in Santa Cruz had a significant effect on the maximum load of the threads while the distal diameter had no effect (ANCOVA, Site $F_{1, 61} = 5.955$, $p < 0.05$; Distal diameter $p > 0.05$).

Table 5. Statistics results from an ANCOVA controlling for thread morphometrics, proximal diameter, distal diameter, thread length, and thread number to assess whether the maximum load of the byssal threads would still be different across collection dates and different between sites for both locations. Table 5a contains statistics for the Santa Cruz location and Table 5b contains statistics for the Pacific Grove location. In the P column, ns stands for not significant. SS stands for sum of squares.

a.

Santa Cruz ANCOVA	df	SS	F	P
Proximal diameter				
Proximal diameter	1	0.120	0.292	ns
Site	1	2.568	6.223	<0.05
Collection date	3	0.508	0.411	ns
Residuals	61	25.167		
Distal diameter				
Distal diameter	1	0.120	0.291	ns
Site	1	2.457	5.955	<0.05
Collection date	3	0.476	0.385	ns
Residuals	61	25.167		
Thread length				
Thread length	1	0.032	0.077	ns
Site	1	2.922	7.057	<0.05
Collection date	3	0.527	0.424	ns
Residuals	61	25.256		
Thread number				
Thread number	1	0.391	0.958	ns
Site	1	2.815	6.897	<0.05
Collection date	3	0.476	0.389	ns
Residuals	61	24.897		

b.

Pacific Grove ANCOVA	df	SS	F	P
Proximal diameter				
Proximal diameter	1	0.107	0.265	ns
Site	1	0.292	0.724	ns
Collection date	2	3.354	4.165	<0.05
Residuals	50	20.134		
Distal diameter				
Distal diameter	1	0.057	0.141	ns
Site	1	0.321	0.795	ns
Collection date	2	3.999	4.953	<0.05
Residuals	50	20.184		
Thread length				
Thread length	1	0.476	1.204	ns
Site	1	0.533	1.348	ns
Collection date	2	4.071	5.15	<0.01
Residuals	50	19.764		
Thread number				
Thread number	1	0.382	0.962	ns
Site	1	0.463	1.166	ns
Collection date	2	4.163	5.24	<0.01
Residuals	50	19.858		

Linear regressions were run to determine if there was an association between the estimated wave heights in the time period preceding each collection event and the maximum load of the mussel threads processed from each collection date. Wave height averages were calculated using the MOP model's predicted nearshore wave heights for three different time periods preceding each collection event. The time periods included wave height averages from, one day before, one week before, and one month before each collection event. These wave height averages were compared against the average maximum load of mussel threads collected during a collection date at a particular site. For both Pacific Grove sites, Pacific Grove Marine Gardens and Point Cabrillo, there was no association between maximum load and the month, week, and wave height averages preceding the collection. The Lighthouse Beach site in Santa Cruz had a positive association between the average wave height a month before the mussel collections and the maximum load of the mussel threads. Wave height predictions from a day before each collection date also had a positive association with the mussel thread's maximum load (Linear regression, Day $F_{1,2}$ = 249, $p < 0.01$, $r^2 = 0.992$, y = 1.626 + 0.367 (day avg wave height)) but the week before did not. The Cowell Beach site in Santa Cruz did not have an association between the maximum load of the mussel byssal threads and any of the average wave heights time periods.

Mussel Morphometrics

Mussel morphometrics measured for all mussels collected include mussel length, maximum width, maximum thickness, and wet weight (Table 6). Statistical tests comparing mussel morphometrics parameters across site and collection date are included in Table 7a for Santa Cruz and Table 7b for Pacific Grove. For the Santa Cruz sites, mussel length, maximum width, and wet weight measurements were larger at Lighthouse Field Beach (Table 6) than Cowell Beach. Lighthouse Field Beach had a higher average maximum thickness than Cowell Beach, but the difference was not significant. All mussel morphometrics varied across the collection dates. Mussel length and wet weight increased with time from the July to the January collection date. Mussel maximum width and thickness increased from July to October but then both decreased from October to January. All four metrics

Table 6. Mean and standard deviation of mussel morphometrics including mussel length, maximum width, maximum thickness and wet weight for the Santa Cruz sites, Cowell Beach(low wave exposure) and Lighthouse Field Beach(high wave exposure), and Pacific Grove sites, Point Cabrillo(low) and Pacific Grove Marine Garden(high).

Site	Mussel length (mm)	Maximum width (mm)	Maximum thickness (mm)	Wet weight (g)
Santa Cruz				
Cowel Beach	55.732 ± 4.989	25.915 ± 2.743	23.854 ± 2.448	17.780 ± 5.355
Lighthouse Field Beach	61.04 ± 7.081	27.363 ± 3.166	24.225 ± 3.921	20.775 ± 9.158
Pacific Grove				
Point Cabrillo	60.167 ± 7.133	28.833 ± 2.805	24.317 ± 2.964	20.1 ± 7.540
Pacific Grove Marine Gardens	59.463 ± 7.951	28.63 ± 2.915	24.775 ± 3.442	20.575 ± 8.661

Table 7. Statistics results from a 2-way ANOVA looking at the difference in site, collection date, and the interaction of site and collection date for the mussel morphometrics, mussel length, maximum width, maximum thickness and wet weight. Table 7a contains statistics for the Santa Cruz location and Table 7b contains statistics for the Pacific Grove location. In the P column, ns stands for not significant. MS stands for mean squares.

a.

Santa Cruz 2-Way ANOVA	df	MS	F	P
Length				
Site	1	570.5	23.276	<0.001
Date	3	181.6	7.406	<0.001
Site x Date	3	205.7	8.39	<0.001
Residuals	73	24.5		
Maximum width				
Site	1	42.44	7.052	<0.01
Date	3	40.21	6.681	<0.001
Site x Date	3	43.98	7.307	<0.001
Residuals	73	6.02		
Maximum thickness				
Site	1	2.79	0.463	ns
Date	3	60.95	10.1	<0.001
Site x Date	3	71.91	11.917	<0.001
Residuals	73	6.03		
Wet weight				
Site	1	181.6	5.552	<0.05
Date	3	445.7	13.629	<0.001
Site x Date	3	231.2	7.07	<0.001
Residuals	73	32.7		

b.

Pacific Grove 2-Way ANOVA	df	MS	F	P
Length				
Site	1	8.5	0.295	ns
Date	2	949	32.945	<0.001
Site x Date	2	100	3.471	<0.05
Residuals	64	28.8		
Maximum width				
Site	1	0.66	0.143	ns
Date	2	132.21	28.786	<0.001
Site x Date	2	0.65	0.142	ns
Residuals	64	4.59		
Maximum thickness				
Site	1	3.6	0.638	ns
Date	2	166.12	29.427	<0.001
Site x Date	2	11.6	2.055	ns
Residuals	64	5.65		
Wet weight				
Site	1	3.9	0.096	ns
Date	2	966.2	23.897	<0.001
Site x Date	2	27.3	0.674	ns
Residuals	64	40.4		

generally increased with time at the Cowell Beach site but for the Lighthouse Field Beach site, mussel morphometrics increased from July to October and then decreased in January. All mussel morphometrics for Santa Cruz had an interaction between site and the collection date.

For the Pacific Grove mussels, there was no difference in site but there was a different across collection date, similar to the thread morphometrics and tensiometer measurements. All thread morphometrics increased over time. The mussel lengths were largest in January compared to August and October (Tukey HSD, $p < 0.0001$).

The maximum width measurements were also larger in January than in August and October (Tukey HSD, $p < 0.0001$) and October has larger width than in August(Tukey HSD, $p < 0.01$). Mussel maximum thickness and wet weight measurments were larger in January than in August and October (Tukey HSD, $p < 0.0001$). Mussel length was the only measurement that had a interaction between site and date for the Pacific Grove mussels.

After controlling for mussel length, maximum width, maximum thickness, and wet weight, in Santa Cruz, site remained as a significant effect on the maximum load of the byssal threads (Table 8a). Lighthouse Field Beach had a higher maximum load than Cowell Beach regardless of mussel size (Tukey, length, $p < 0.05$; width, $p < 0.05$; thickness, $p < 0.01$; wet weight, $p < 0.05$). In Pacific Grove, after accounting for mussel size, collection date did not have a significant effect on the maximum load of the byssal threads (Table 8b) as also seen in the uncorrected data.

There were more significant correlations between the mussel and thread parameters at the Pacific Grove location compared to the Santa Cruz location (Table 9). From the Pacific Grove Marine Gardens data (Table 9c), there was a negative correlation between thread number and all of the mussel morphometric

Table 8. Statistics results from an ANCOVA controlling for mussel morphometrics, mussel length, maximum width, maximum thickness and wet weight to see if the maximum load of the byssal threads would still be different across collection dates and different between sites for both locations. Table 8a contains statistics for the Santa Cruz location and Table 8b contains statistics for the Pacific Grove location. In the P column, ns stands for not significant. SS stands for sum of squares.

a.

Santa Cruz ANCOVA	df	SS	F	P
Mussel length				
Mussel length	1	0.698	1.73	ns
Site	1	1.691	4.194	<0.05
Collection date	3	0.140	0.116	ns
Residuals	61	24.590		
Maximum width				
Maximum width	1	1.477	3.785	ns
Site	1	1.937	4.961	<0.05
Collection date	3	0.0445	0.038	ns
Residuals	61	23.810		
Maximum thickness				
Maximum thickness	1	1.107	2.793	ns
Site	1	3.010	7.593	<0.01
Collection date	3	0.091	0.077	ns
Residuals	61	24.181		
Wet weight				
Wet weight	1	0.686	1.702	ns
Site	1	2.502	6.204	<0.05
Collection date	3	0.031	0.026	ns
Residuals	61	24.601		

b.

Pacific Grove ANCOVA	df	SS	F	P
Mussel length				
Mussel length	1	1.730	4.673	<0.05
Site	1	0.219	0.591	ns
Collection date	2	0.650	0.878	ns
Residuals	50	18.510		
Maximum width				
Maximum width	1	1.598	4.285	<0.05
Site	1	0.230	0.618	ns
Collection date	2	1.078	1.445	ns
Residuals	50	18.643		
Maximum thickness				
Maximum thickness	1	0.661	1.687	ns
Site	1	0.133	0.338	ns
Collection date	2	1.408	1.798	ns
Residuals	50	19.579		
Wet weight				
Wet weight	1	1.280	3.375	ns
Site	1	0.148	0.389	ns
Collection date	2	1.412	1.862	ns
Residuals	50	18.960		

measurements. The proximal diameter measurements from mussel threads from Pacific Grove Marine Gardens was positively correlated with mussel length and mussel maximum thickness. From the Point Cabrillo site (Table 9d), the proximal diameter measurements were positively correlated with mussel length, maximum thickness and wet weight. The distal diameter measurements were positively correlated with mussel maximum thickness and thread length at Point Cabrillo was negatively correlated to mussel length. At the Santa Cruz location, there was a positive correlation between distal diameter and mussel maximum thickness at the Lighthouse Field Beach site (Table 9a) and there was a positive correlation between thread number and mussel length at the Cowell Beach site (Table 9b).

Table 9. Spearman's correlations between mussel morphometrics, including mussel length, maximum width, maximum thickness, and wet weight, and thread morphometrics, including proximal diameter, distal diameter, thread length and thread number at (a) Lighthouse Field Beach, (b) Cowell Beach, (c) Pacific Grove Marine Gardens, and (d) Point Cabrillo. For each significant result the p value and correlation coefficient rho are included, 'ns' was used to indicate that the correlation was not significant.

a.

Lighthouse Field Beach	Mussel length	Maximum width	Maximum thickness	Wet weight
Proximal diameter	ns	ns	ns	ns
Distal diameter	ns	ns	$p < 0.05$, rho = 0.357	ns
Thread length	ns	ns	ns	ns
Thread number	ns	ns	ns	ns

b.

Cowell Beach	Mussel length	Maximum width	Maximum thickness	Wet weight
Proximal diameter	ns	ns	ns	ns
Distal diameter	ns	ns	ns	ns
Thread length	ns	ns	ns	ns
Thread number	$p < 0.01$, rho = 0.445	ns	ns	ns

c.

Pacific Grove Marine Gardens	Mussel length	Maximum width	Maximum thickness	Wet weight
Proximal diameter	$p < 0.05$, rho = 0.470	ns	$p < 0.05$, rho = 0.387	ns
Distal diameter	ns	ns	ns	ns
Thread length	ns	ns	ns	ns
Thread number	$p < 0.0001$, rho = -0.676	$p < 0.001$, rho = -0.629	$p < 0.001$, rho = -0.665	$p < 0.001$, rho = 0.387

d.

Point Cabrillo	Mussel length	Maximum width	Maximum thickness	Wet weight
Proximal diameter	$p < 0.05$, rho = 0.381	ns	$p < 0.01$, rho = 0.519	$p < 0.05$, rho = 0.415
Distal diameter	ns	ns	$p < 0.05$, rho = 0.415	ns
Thread length	$p < 0.001$, rho = -0.045	ns	ns	ns
Thread number	ns	ns	ns	ns

Discussion

The idea that organisms build physical structures to withstand not only average environmental stress but also episodic maxima is widely supported. Some of these physical structures include spider silk (Xu and Lewis, 1990), sandcastle worm tubes (Stewart et al., 2011), along with mussel byssal threads. Overall, results from this study were consistent with that paradigm. However, mussels from the two locations appeared to respond to different types of wave exposure gradients. In Santa Cruz, mussels in the site of presumed higher wave exposure had stronger byssal threads. In the other location, Pacific Grove, this was not the case. However, mussels in Pacific Grove altered thread morphology and strength across seasons, showing they were capable of plasticity in thread shape. Differences in response to estimated wave energy between Santa Cruz and Pacific Grove suggest the potential influence of additional factors, such as thread degradation or regeneration rates, reproductive cycles, or seasonal temperature changes. Although there were differences in thread strength, across date in Pacific Grove and between sites in Santa Cruz, the differences were not influenced by thread thickness, meaning thread compositional differences and or environmental factors were at play. Too, wave force estimated by measurement or models may have been too coarse to predict forces felt by individual mussels. These complexities are discussed below.

Environmental Data

Unfortunately, wave dynamometers did not withstand the rigors of the rocky intertidal zone, so wave force was estimated by modeling. Although the model was able to provide context for the wave forces at each site, the data used to model wave force were taken at a large scale relative to size of individual mussels. The different environments at each location appeared to affect how well the MOPs model predicted near shore wave heights. The MOPs model was developed specifically for estimating near shore wave height in the sandy environments of San Clemente in southern California (O'Reilly et al., 2016). The Santa Cruz sites were located in a sandy environment, and the MOPs model should have a higher success of estimating nearshore wave heights in Santa Cruz. The Pacific Grove location is rocky which lowers the skill of the model's predictions because of the complex topography. O'Reilly et al. (2016) identified Point Cabrillo as an area were the MOPs model struggled to estimate nearshore wave heights due to this site being highly sheltered and rocky.

Regardless of the skill of the MOPS model, nearshore wave height does not guarantee a correct estimation of the wave velocity in the intertidal zone. In a study by Helmuth and Denny (2003) in Pacific Grove, nearshore wave height measurements were compared to the wave forces that were measured at microsites in the rocky intertidal at Point Cabrillo to see if the variables were correlated. In the majority of these sites, force increased nonlinearly to a defined limit, likely caused by wave breaking. Nearshore wave breaking diminishes the energy of a wave through turbulent dissipation (Denny, 1995) and localized topography can further dissipate the wave forces making it difficult to predict the wave forces felt by individual organisms in the intertidal.

Since dynamometers measure forces at a scale more relevant to mussels, a more robust dynamometer should be used to assess the wave velocity experienced by the individual mussels. Designs subsequent to Bell and Denny (1994) anchor the body of the dynamometer in a hole drilled into the substrate so that only the drogue is subjected to the wave forces, reducing the risk of dislodgement. Current sensor technologies and on-board data storage may allow smaller and shapeable instruments that mimic shells and better characterize forces felt by living mussels.

Thread Composition

In Santa Cruz, at the exposed site, Lighthouse Field Beach, mussels had thicker proximal and distal byssal thread regions than at the more protected site, Cowell Beach. This result supports the hypothesis that higher wave exposure will cause adaptions for survival like the thickening of byssal threads which may lead to stronger threads (Carrington, 2002). In Pacific Grove, there was no difference in the thread morphometrics between sites, but instead there was a difference across collection dates for proximal and distal diameter and thread length and thread number. Although this result was unexpected because of the large difference in estimated near shore wave height at the two Pacific Gove sites, the inaccuracy of the MOPs model in rocky habitats in combination with the dissipation of wave velocity in complex topography of these sites, made the measurements of wave exposure less reliable, as discussed above. The increase in the diameter of the thread's proximal and distal regions provides evidence that seasonal fluctuations in the mussels' energy allocation influence thread morphometrics, while the effects of wave force were location specific.

The thread strength from both Santa Cruz and Pacific Grove followed a similar pattern to the thread morphometrics. In Santa Cruz, there was a difference in maximum load between sites with Lighthouse Field Beach having higher maximum load measurements than Cowell Beach. In Pacific Grove, there was no difference in maximum load between sites but there was a difference across collection dates with the maximum load increasing over time. Although these results seem to point to the increase in thread strength being related to the increase in thread diameter, this is not the case. After controlling for proximal and distal diameters for Santa Cruz threads, site still had an influence on the maximum load of the threads but the diameter of the threads did not. Similarly in Pacific Grove, after controlling for the thread morphometrics, the collection date still influenced the thread strength but the thread dimensions and number did not. This suggests that there are changes to the threads composition independent of diameter that could be affecting thread strength. Byssal threads have been shown to have amino acid composition that varies with external or biological factors like water flow (McDowell et al., 1999), food availability, or spawning (Babarro and Fernández Reiriz, 2010). Specific amino acids like histidine and lysine provide sites for metal chelation which can help threads endure stronger forces and recover after undergoing tension. In a study by Babarro and Fernández Reiriz (2010), threads from mussels that were forced to spawn had high concentrations of histidine and lysine residues present compared to other treatments where mussels did not spawn or were left unfed. Babarro and Fernández Reiriz (2010) argued that this increase in histidine and lysine could aid the mussel in staying anchored when their byssal thread production decreases after spawning. The histidine and lysine would create more sites for metal chelate binding creating stronger and stiffer threads and increasing the likelihood of the mussel maintaining attachment to the substrate.

Thread Strength vs Tenacity

In this study, individual thread strengths were analyzed to determine if wave forces had an effect on the individual threads. Typically, individual mussel threads have been produced in lab conditions for study, with a few exceptions that were collected from natural sites (e.g. Babarro and Carrington, 2011). Tenacity has been used to see how much force is needed to dislodge a mussel in nature because the whole byssus is more relevant to maintaining attachment than the strength of a singular thread. Although this study did not fully support a relationship between site-related wave exposure and thread strength (i.e, in Pacific Grove), it may be possible that the tenacity of mussel from this study do mirror the wave exposure levels of each site. Wave forces are a driving factor in mussel tenacity (Carrington, 2002), but there are biological factors also at play. Each year mussels spawn and the formation of gonads causes a change in energy allocation. Energy is redistributed from thread production to gonad production in preparation for a spawning event (Carrington, 2002). After this spawning event, typically in spring, the increase in temperature also impacts the degradation of threads. In summer months, thread production increases but the threads are off a lower quality meaning that individual threads are less strong than those produced in spring months (Moeser et al., 2006).

Conclusion

The hypotheses, which were formulated around site differences in wave energy, were supported in Santa Cruz: higher thread strength and thickness was observed at the more wave exposed site, Lighthouse Field Beach, compared to the less exposed site Cowell Beach. If the wave gradient is seasonal, the hypotheses were supported in Pacific Grove: differences in thread strength and thickness were seen as wave energy increased from summer to winter. However, even with this *post-facto* rearrangement of the hypotheses, the inconsistency across sites in response to inferred site-related and seasonal shifts in wave energy suggests either inaccurate estimation of wave energy (due to limitations of the MOPs model), or that wave energy alone cannot fully explain byssal thread biomechanics. In future studies, wave forces measured on mussel mimics would better classify exposure levels relevant to mussels. With better wave force data, other factors, such seasonal energy allocation, can be systematically investigated. This study clearly showed variability in byssal thread strength and morphology for *Mytilus californianus* across sites and seasons. The extent to which this was an adaptive response to wave energy gradients awaits more precise physical measurements of waves in the field.

REFERENCES

Babarro, J. M. F.; Carrington, E. Byssus secretion of *Mytilus galloprovincialis*: effect of site at macro- and micro-geographical scales within Ría de Vigo (NW Spain). *Mar. Ecol.: Prog. Ser.* **2011**, *435*, 125–140.

Babarro, J. M. F.; Fernández Reiriz, M. J. Secretion of byssal threads in Mytilus galloprovincialis: Quantitative and qualitative values after spawning stress. *J. Mar. Biol. Assoc. U. K.* **2010**, *180*, 95–104.

Bell, E. C.; Denny, M. W. Quantifying “wave exposure”: a simple device for recording maximum velocity and results of its use at several field sites. *J. Exp. Mar. Biol. Ecol.* **1994**, *181*, 9–29.

Bell, E. C.; Gosline, J. M. Strategies for life in flow: Tenacity, morphometry, and probability of dislodgment of two Mytilus species. *Mar. Ecol.: Prog. Ser.* **1997**, *159*, 197–208.

Bell, E. C.; Gosline, J. M. Mechanical design of mussel byssus: Material yield enhances attachment strength. *J. Exp. Biol.* **1996**, *199*, 1005–1017.

Bouhlel, Z.; Genard, B.; Ibrahim, N.; Carrington, E.; Babarro, J. M. F.; Lok, A.; Flores, A. A. V.; Pellerin, C.; Tremblay, R.; Marcotte, I. Interspecies comparison of the mechanical properties and biochemical composition of byssal threads. *J. Exp. Biol.* **2017**, *220*, 984-994.

Brazee, S. L.; Carrington, E. Interspecific Comparison of the Mechanical Properties of Mussel Byssus. *Biol. Bull. (Chicago, IL, U. S.).* **2006**, *211*, 263-274.

Brown, C. H. Some Structural Proteins of *Mytilus edulis*. *Q. J. Microsc. Sci.* **1952,** *93* (4), 487–502.

Carrington, E. Seasonal Variation in the Attachment Strength of Blue Mussels : Causes and Consequences. *Limnol. Oceanogr.* **2002**, *47* (6), 1723–1733.

Denny, M. Predicting Physical Disturbance: Mechanistic Approaches to the Study of Survivorship on Wave-Swept Shores. *Ecol. Monogr.* **1995**, *65*, 371-418.

Erikson, Li H.; Storlazzi, Curt D.; Golden, Nadine E. Wave Height, Peak Period, and Orbital Velocity for the California Continental Shelf. U. S. Geological Survey data set, **2014**. DOI: 10.5066/F7125QNQ

Harrington, M. J.; Waite, J. H. Holdfast heroics: comparing the molecular and mechanical properties of *Mytilus californianus* byssal threads. *J. Exp. Biol.* **2007**, *210*, 4307–4318.

Harrington, M. J.; Gupta, H. S.; Fratzl, P.; Waite, J. H. Collagen insulated from tensile damage by domains that unfold reversibly: In situ X-ray investigation of mechanical yield and damage repair in the mussel byssus. *J. Struct. Biol.* **2009**, *167*, 47–54.

Harrington, M. J.; Masic, A.; Holten-Andersen, N.; Herbert Waite, J.; Fratzl, P. Iron -Clad Fibers: A Metal-Based Biological Strategy for Hard Flexible Coatings. *Science*. **2010**, *328*, 216–220.

Helmuth, B.; Denny, M. W. Predicting wave exposure in the rocky intertidal zone: Do bigger waves always lead to larger forces? *Limnol. Oceanogr*. **2003**, *48*. 1338 -1345

Lucas, J. M.; Vaccaro, E.; Waite, J. H. A molecular, morphometric and mechanical comparison of the structural elements of byssus from *Mytilus edulis* and *Mytilus galloprovincialis*. *J. Exp. Biol.* **2002**, *205*, 1807–1817.

McDowell, L. M.; Burzio, L. A.; Waite, J. H.; Schaefer, J. Rotational Echo Double Resonance Detection of Cross-links Formed in Mussel Byssus under High-Flow Stress. *J. Biol. Chem.* **1999**, *274*. 20293-5.

Moeser, G. M.; Leba, H.; Carrington, E. Seasonal influence of wave action on thread production in Mytilus edulis. *J. Exp. Biol.* **2006**, *209*, 881–890.

O'Reilly, W. C.; Olfe, C. B.; Thomas, J.; Seymour, R. J.; Guza, R. T. The California coastal wave monitoring and prediction system. *Coastal Eng*. **2016**, *116*, 118 -132.

Qin, X.; Waite, J. H. Exotic collagen gradients in the byssus of the mussel *Mytilus edulis*. *J. Exp. Biol.* **1995**, *198* (3), 633–644.

Qin, X.-X.; Coyne, K. J.; Waite, J. H. Tough Tendons: Mussel byssus has collagen with silk-like domains. *J. Biol. Chem.* **1997**, *272* (51), 32623- 32627.

Stewart, R. J.; Wang, C. S.; Shao, H. Complex coacervated as a foundation for synthetic underwater adhesives. *Adv. Colloid Interface Sci.* **2011**, *167* (1-2), 85 -93.

Sun, C.; Waite, J. H. Mapping Chemical Gradients within and along a Fibrous Structural Tissue, Mussel Byssal Threads. *J. Biol. Chem.* **2005**, *280* (47), 39332 -39336.

Vaccaro, E.; Waite, J. H. Yield and Post-Yield Behavior of Mussel Byssal Thread: A Self-Healing Biomolecular Material. *Biomacromolecules*. **2001**, *2*, 906-911.

Waite, H.; Qin, X.-X.; Coyne, K. The Peculiar Collagens of Mussel Byssus. *Matrix Biol.* **1998**, *17*, 93-106.

Wang, J.; Scheibel, T. Recombinant Production of Mussel Byssus Inspired Proteins. *Biotechnol. J.* **2018**, 1800146, 1-12.

Witman, J. D.; Suchanek, T. H. Mussels in flow: drag and dislodgement by epizoans. *Mar. Ecol. Prog. Ser.* **1984**, *16* (3), 259–268.

Xu M.; Lewis R. V. Structure of a protein superfiber: spider dragline silk. *Proc. Natl. Acad. Sci. U.S.A.* **1990**, *87* (18), 7120–7124.

APPENDIX

Dynamometer construction

The construction of the dynamometers followed Bell and Denny (1994). The dynamometers were made up of a spring housed in a CPVC tube. One side of the spring was secured inside of a sealed side of the tube and the other side of the spring had a fishing line connected to it that extended through a channel outside of the tube. A piece of rubber was threaded onto the fishing line inside the tube. The size of the rubber piece was bigger than the channel where the fishing line exits the tube so that it moved on the fishing line as the spring extended. This rubber marker was used to measure maximum spring extension over a given time period that was used to calculate the maximum wave velocity. The fishing line was tied to a practice golf ball outside of the tube which acted as a drogue. At each of the collection sites, 3 dynamometers were bolted to the substrate by a swivel to allow the dynamometer to rotate freely. As the waves washed over the dynamometer, the practice golf ball was pulled by the waves and the spring inside the dynamometer extended. The rubber marker inside the CPVC housing was moved towards the spring on the fishing line corresponding to the extension of the spring which was used to calculate the maximum wave velocity at each site. To calibrate the dynamometers before deployment, 5 known masses were hung from the dynamometers and the extension of the springs was recorded. These extension measurements were converted to units of force by multiplying the acceleration due to gravity ($9.81 m/s^2$). These forces were plotted to create linear regression of force vs extension,

$$F = kx + c,$$

where k is the spring constant, x is the extension of the spring, and c is the force needed to overcome the initial compression of the spring. The measurements of force from drag on the practice golf ball was taken from Bell and Denny (1994). In their study, they used a unidirectional flow tank to subject their practice golf balls to known water velocities ranging from 0.5 to 3 m/s. Bell and Denny's (1994) calculations were used because the practice golf balls in this study have the same dimensions as the ones they used. The measurements of drag on Bell and Denny's (1994) practice golf balls were fitted on to the following power curve,

$$F_d = au^b,$$

where the a and b constants were calculated to be 0.575 and 1.93. These two equations can then be combined into the following equation to calculate wave velocity based on the spring extension measurements taken from collection sites:

$$u = \left(\frac{kx+c}{a}\right)^{\frac{1}{b}}.$$

The dynamometers were deployed in July 2019 at the start of mussel collections until November 2019. During each successive collection event, the extension of the spring was measured from each dynamometer and recorded. After recording the spring extension, the rubber marker was reset for the next collection event.